

Spin transport in dangling-bond wires on doped H-passivated Si(100)

Mikaël Kepenekian^{1,2}, Roberto Robles^{2,3}, Riccardo Rurali⁴,
Nicolás Lorente^{2,3}

¹Institut des Sciences Chimiques de Rennes UMR 6226, CNRS - Université de Rennes 1, Rennes, France

²ICN2 - Institut Català de Nanociència i Nanotecnologia, Campus UAB, 08193 Bellaterra (Barcelona), Spain

³CSIC - Consejo Superior de Investigaciones Científicas, ICN2 Building, Campus UAB, 08193 Bellaterra (Barcelona), Spain

⁴Institut de Ciència de Materials de Barcelona (ICMAB-CSIC), Campus de Bellaterra, 08193 Bellaterra (Barcelona), Spain

E-mail: mikael.kepenekian@univ-rennes1.fr

Abstract. New advances in single-atom manipulation are leading to the creation of atomic structures on H passivated Si surfaces with functionalities important for the development of atomic and molecular based technologies. We perform total-energy and electron-transport calculations to reveal the properties and understand the features of atomic wires crafted by H removal from the surface. The presence of dopants radically change the wire properties. Our calculations show that dopants have a tendency to approach the dangling-bond wires, and in these conditions, transport is enhanced and spin selective. These results have important implications in the development of atomic-scale spintronics showing that boron, and to a lesser extent phosphorous, convert the wires in high-quality spin filters.

PACS numbers: 73.63.Nm,73.20.-r,75.70.-i

Submitted to: *Nanotechnology*

1. Introduction

The integration of semiconductors and magnetic materials is of great importance for the creation of new technology in which digital data are encoded in the spin of electrons. [1] To this respect, the use of molecules that can become spin devices is a very interesting possibility. [2] Indeed, molecular devices are very small, adaptable and easy to create using chemical engineering. Their spin functionalities are also very interesting, and they have been deemed superior to more common spintronic strategies. [3, 4] As in molecular electronics, [5, 6] the problem still comes from creating efficient atomic-size interconnects to form complete circuits. [6, 7]

Interconnects that can transport spin are then desirable for spintronic application. Promising candidates for surface interconnects can be found in carbon nanotubes (CNTs), [8, 9] as they present both easy synthesis and complex physics. In particular, the low Z of carbon, assures very small spin-orbit coupling and hence long spin lifetimes. However, an important issue with CNTs is that their properties are extremely sensitive to the topological structure of the tube. Other serious candidates emerge from the variety of silicon nanowires (Si NWs) that can be grown and that happen to present an easier control on their physical properties. [10, 11] A new type of nanowires has been recently proposed with embedded phosphorous in a silicon crystal. The resulting 1-D system exhibits then a very low resistivity. [12] An alternative path consists in using the scanning tunneling microscope (STM) to selectively remove hydrogen atoms from a H-passivated Si(100) surface along the Si dimer row leading to a dangling-bond (DB) wire. [13, 14, 15, 16, 17, 18, 19] At variance with isolated DBs, which introduce localized mid-gap states, these wires give rise to dispersive bands with a marked one-dimensional character. The stability and the transport properties of such wires have been extensively studied by tight-binding as well as *ab initio* methods [20, 21, 22, 23, 24, 25, 26, 27, 28, 29, 30, 31] and several experimental proofs-of-concept have been reported. [15, 16, 32]. Spin lifetimes in silicon are known to be long, however DB wires present some problems for transport: (*i*) transport properties of simple 1-D wires are limited due to the appearance of an electronic gap, [31, 7] and (*ii*) the coupling of the wire with the substrate due to the presence of dopants and impurities leads to a leak of the electronic current in the bulk. [33]

In the present work we focus on the effect of dopants, boron (*p*-type) and phosphorous (*n*-type), on the electronic transport properties of DB-wires with special interest in the spin transport properties. In a semiconductor, the density of carriers can be tuned by adding dopants. In a conventional approach, DBs are undesired surface defects, because they introduce deep states in the band-gap that act as charge traps, reducing the conductivity. Here, we place ourselves in the opposite situation: DB conductive wires are engineered on a Si surface, for a specific purpose, e.g. transporting charge and spin between two devices, and we focus on how dopants affect transport in these wires. We start by analyzing the dopant segregation on the H-passivated Si(100) surface with and without DB wires, finding that dopants segregate at the surface. Next,

we observe two remarkable effects of the dopants: first, dopants greatly reduce the gap, which leads to quasi-metallic wires; second, as they stabilize the magnetic ordering in the wires, the wire transport becomes spin polarized. We find that DB-wires are good spin filters, going beyond simple interconnects. Hence, DB wires will not only transport spin, but will make sure that the spin polarisation is preserved.

2. Computational details

First-principles calculations are based on density functional theory (DFT) as implemented in the SIESTA package. [34, 35] Calculations have been carried out with the GGA functional in the PBE form, [36] Troullier-Martins pseudopotentials, [37] and a basis set of finite-range numerical pseudoatomic orbitals for the valence wave functions. [38] Structures have been relaxed using a double- ζ polarized basis sets. [38] The surfaces were modeled using a slab geometry with eight silicon layers and a 4×8 unit cell of the H-passivated Si(100)-(2 \times 1) surface. The extent of the cell allows one to limit the direct interaction between dopants, but still leads to a very high concentration of dopant with one Si atom out of 600 being substituted by a B or P atom. The electronic structure was converged using a $1 \times 5 \times 5$ k -point sampling of the Brillouin zone. Conductances have been computed using a single- ζ polarized basis set, by means of the TRANSIESTA method, [39] within the non-equilibrium Green's function (NEGF) formalism. The following setup has been used: 4-dimer DB wires act as left and right electrodes, while a 8-dimer DB wire constitutes the scattering region. The current is evaluated following Landauer's equation: [40]

$$I = \frac{2e}{h} \int_{-\infty}^{\infty} T(E, V) [f_R(E) - f_L(E)] dE$$

where $T(E, V)$ is the transmission function for an electron of energy E when the bias between the two DB electrodes is V , and $f_R(E)$ ($f_L(E)$) is the right- (left-) electrode Fermi occupation function. We further simplify the current I calculation using the zero-bias transmissions. In TRANSIESTA, bias between the electrodes is established by applying an electric field along the transport direction. Mobile charges inside the electrodes screen the electric field, resulting in the usual electric potential profile (flat inside the electrodes, potential drop in the scattering region). Only electrodes that are three-dimensional metals guarantee this kind of screening. In this configuration, however, it becomes very difficult to disentangle the contributions to the resistance of the electrode-semiconductor interface from those of the sub-surface dopant scattering. We believe that our simplified model gives a better insight into the physics of electron transport through DB wires in presence of dopant, because all the observed effects (stabilization of a magnetic solution, leakage, ...) necessarily stem from the presence of the impurities. The price to pay is that biased calculation cannot be performed for the methodological reasons outlined above. In all cases, an energy cutoff of 200 Ry for real-space mesh size has been used.

3. Results and discussion

The impact of dopants on the current carried by DB-wires depends critically on their distribution with respect to the surface. Hence, our first goal was studying the surface segregation of these defects. Broadly speaking, we find that in this system impurities prefer to be closer to the surface because the strain introduced can be more easily released. This is a well-known behaviour in similar systems, like unpassivated Si surfaces [41, 42] and in Si nanowires. [43, 44, 11] Our calculations show the same trend in the H-passivated Si(100) surface. For both B and P, nearly 150 meV are gained in the most stable surface position (see Figure 1(b) and Table 1). As the dopant gets closer to the surface, the formation energy becomes much more site-specific. It appears that sites D, E and F are favored with respect to sites A, B and C, respectively. These differences vanish quickly moving away from the surface and are within the numerical accuracy of the calculation at 15 Å from the surface. In the following, we limit our discussion to the case of a substitution at sites D, E and F which appears to be more stable than those at A, B and C sites.

Table 1. Formation energies (in meV, see text) for sites D, E, and F with and without DB-wires. The notations X@H-passivated, X@NM and X@AFM stands for a system with the dopant X (X=B, P) below a H-passivated surface, a NM and AFM wire, respectively.

	D	E	F
B@H-passivated	29	-148	214
B@NM	-14	-415	-12
B@AFM	-10	-110	-123
P@H-passivated	-61	-145	105
P@NM	-237	-488	-57
P@AFM	-329	-539	-180

The site selectivity observed in Figure 1(b) depends on several intertwined factors (strain relaxation, electronic states of the neighbouring DBs...), but can be roughly tracked back to the amount of charge transfer by the dopant depending on the site substituted. We find that the most stable site corresponds to the largest charge transfer, *i.e.* to the strongest bond form between the dopant and its Si neighbours (see Figure 1(c)).

Starting from the previous structures, DB-wires are *drawn* on the surface by removing a row of Hydrogens along the [110] direction. In the absence of dopants, such wires are known to be unstable and relax following either a non-magnetic (NM) Peierls distortion or a spin-polarized solution that leads to antiferromagnetic (AFM) ordering. [20, 21, 23, 24, 25, 26, 27, 29, 30] The two solutions are very close in energy with the NM configuration more stable than the AFM one by 5 meV/DB. [30]

Our results show that surface segregation is enhanced by the presence of such DB-

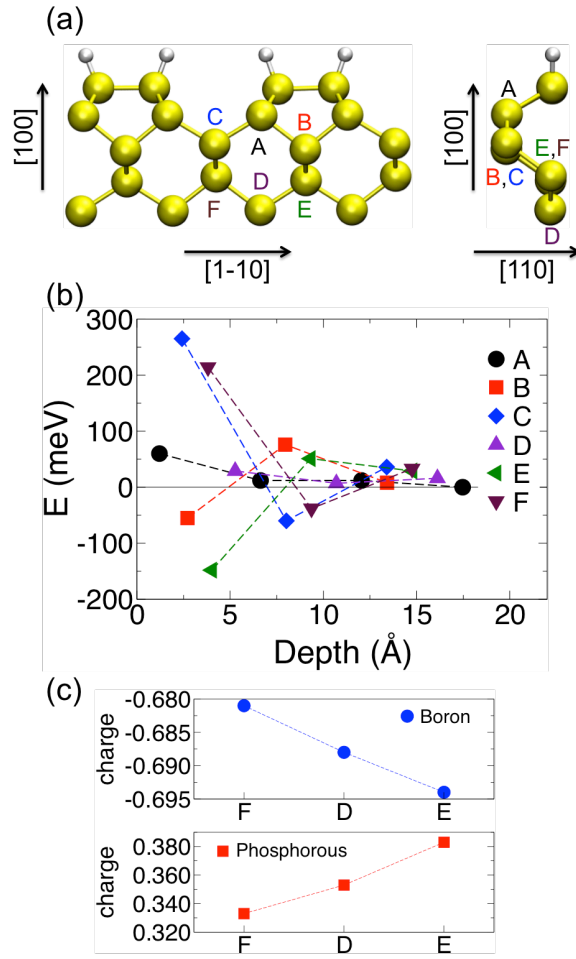


Figure 1. (a) Side views of the H-passivated Si(100) surface, where the dimers formed on the surface can be seen on the upper part. Si and H atoms are depicted in yellow and white, respectively. The different lattice sites for B and P are indicated. Sites A, B and C are shifted with respect to the surface dimers, whereas sites D, E and F are positioned below them (cf. right side). (b) Formation energies (meV) of boron in Si close to the H-passivated Si(100) surface. At the bulk limit all the sites A, B, C, D, E, and F are equivalent. The corresponding formation energy is taken as a reference. The formation energies become site-specific close to the surface. (c) Calculated Mulliken net charges of the boron and phosphorous impurities depending on the site substituted. Dashed lines are a guide to the eye.

wires. Indeed, whatever the site of substitution for B or P is, the formation energy is smaller than in the bulk position (see Table 1). This is in agreement with previous results on Si NWs, [43, 45] where dopants are found to form electrically inactive complexes with isolated DBs. Also here, the tendency to surface segregation is more pronounced with P, as observed in the case of Si NWs and unpassivated Si(100) surface. [43, 45]

More interestingly, we have found that both B and P stabilize the magnetic solution with respect to the NM distorted one, regardless of the site of substitution (see Table 2). The destabilization of the NM wire is due to the increased distortion caused by the dopant. The shortening going from Si-Si to Si-B or Si-P bonds is conflicting with the

Table 2. Energy differences (in meV/DB) between NM and AFM configurations for top sites D, E, and F. In the absence of dopant this difference is -5 meV/DB. [30]

B@D	B@E	B@F	P@D	P@E	P@F
10	22	16	20	15	21

buckling imposed by the NM Peierls-like structure. As an example the buckling in the non-doped NM structure gives differences of $\Delta z = 0.69$ Å in the vertical direction between neighbour DBs. In a B-doped (P-doped) system, this height difference becomes as high as $\Delta z = 1.34$ Å ($\Delta z = 1.52$ Å) close to the dopant. In the undistorted AFM wire the deformation introduced by the dopant is much less: Δz of 0.16 Å and 0.24 Å for B and P, respectively. The geometry of the magnetic solution is preserved. Thus, in the presence of dopants the AFM solution becomes the ground state, yielding a magnetic ordering that can be exploited for spin transport related applications.

Dopants lead to an injection of hole or electrons. In the presence of DBs on H-passivated Si(100), the extra charges are trapped by these surface defects, leading to a decrease in the conductance. Here, however, where conduction is supposed to take place along the DB-wires, this effect turns out to be positive by closing the electronic gap of the AFM wire and leading to a spin-specific quasi-metallicity.

Figure 2 shows the band structure of (a) an undoped AFM wire, (b) an AFM wire with a substitutional B atom in its most stable configuration (F site) and (c) an AFM wire with a substitutional P atom in its most stable configuration (E site). One can see the expected shifting of the Fermi energy (dashed line) controlled by the amount of extra charge/hole injected in the system through the dopant. The undoped AFM wire, Fig. 2 (a), shows two surface states leaving a surface-band gap of 0.56 eV. For each surfaces state, the bands corresponding to each spin overlap due to the AFM ordering. The B-doped system, Fig. 2 (b), displays a splitting of bands according to spin (red and blue for majority and minority spins). The splitting of bands is due to the introduction of an extra spin in an otherwise perfect AFM wire, leading to an unbalanced number of spins. The increase of the DB charge, also caused by the dopant, produces the reduction of the surface-band gap to 0.05 eV. In the case of P doping, the extra spin also produces the spin polarisation of bands and a 0.09 -eV gap. Therefore, the presence of dopants brings the initial insulating system to a spin-polarized quasi-metallic state.

Figure 3 shows the computed I-V curves for B- and P-doped AFM wires. In both cases, the bias required to obtain a current response is below 0.1 V in agreement with the above electronic gaps. In the case of P doping, the current contains a bulk contribution to the current. This leads to leakage current, *i.e.* a loss of surface current into the Si bulk. A previous study showed that this loss could represent as much as 30% of the total current for low biases (less than 0.5 V). [33] Figure 3 displays the current along the DB wire that does not contain the fraction of the current lost into the bulk. This explains why the current is largely spin polarized despite having a larger number of bulk

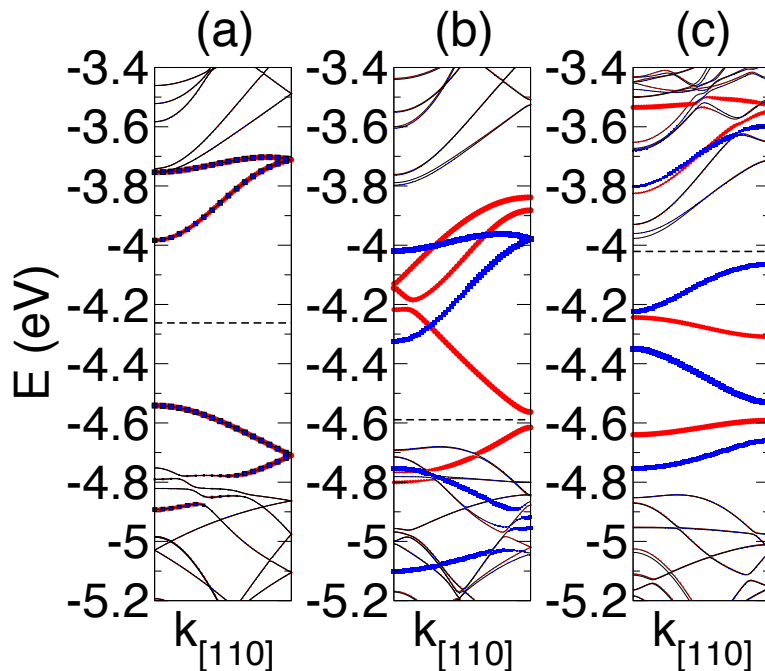


Figure 2. Electronic bands evaluated for a periodic magnetic nanowire with (a) a pure Si substrate, (b) B-doped Si substrate, and (c) P-doped Si substrate. The red and blue circles indicate the weight of the DB in the majority and minority spin bands, respectively. The dashed lines indicate the position of the Fermi energy.

bands, because the wire current is mainly due to the first band below the Fermi energy, which is a surface band and hence spin polarized.

However, current leakage is negligible for B doping because there is no bulk bands in the energy windows for low biases. Indeed, for biases between 0.05 and 0.18 V the current remains on the surface and the current leakage is strictly zero. The spin-polarisation for both dopings is the same, *i.e.* adding or subtracting one electron by the dopant will change the spin balance on the DB, but the majority spin will be the same spin. However, the surface current shows different spin-polarisations, Fig. 3. This is due to the actual ordering of the DB bands, which changes under the dopant potential.

By defining the spin polarisation like $P = (I_{\uparrow} - I_{\downarrow}) / (I_{\uparrow} + I_{\downarrow})$, we obtain that B-doped systems present a 100% polarisation for biases below 0.17 V, Fig. 4. Beyond this bias the presence of bulk bands contribute to current leakage and to the loss of spin polarisation. In the case of P-doped system, the bulk bands contribution starts as early as 0.09 eV, leading to a lower spin polarisation. Therefore, for biases lower than 0.17 V, the B-doped DB wire drawn on H-passivated Si(100) system is a perfect spin-filtering surface interconnect thanks to the absence of current leakage and to the perfect spin polarisation.

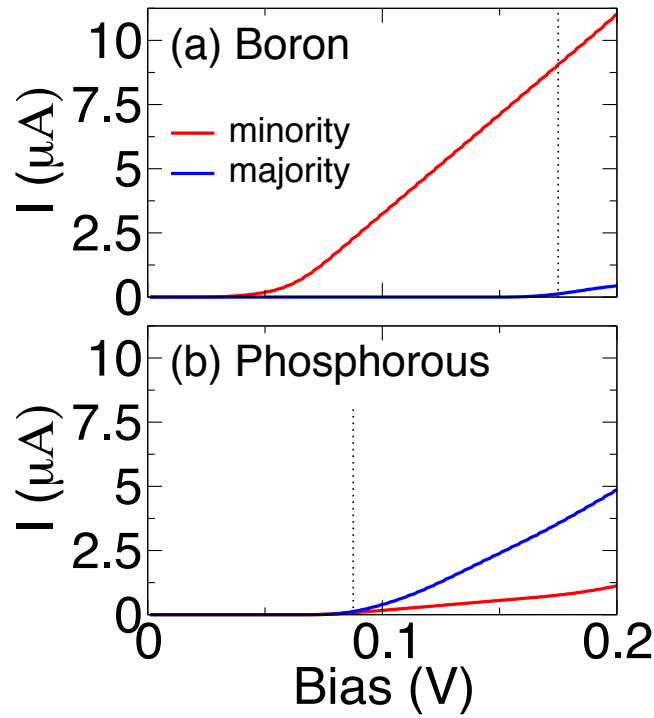


Figure 3. I-V curve for the most stable B-doped (a) and P-doped (b) AFM dangling-bond wire. The dotted black line indicates the bias at which bulk contributions to the current starts. For larger biases, a part of the current is lost into the Si bulk (leakage current). The non-doped AFM DB wire presents a gap larger than the bias window considered here.

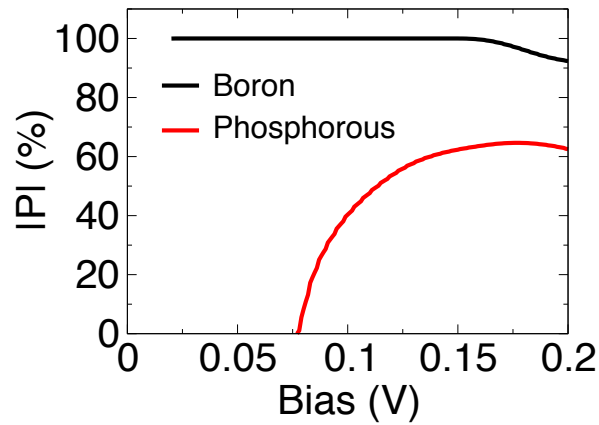


Figure 4. Spin polarisation for the B-doped system (black) and the P-doped one (red). The curves are not defined for biases below the band gaps, since the wires hold no current. B-doped systems show 100% polarisation for biases below 0.17 V. Beyond this bias the presence of bulk bands contribute to current leakage and to the loss of spin polarisation. In the case of P-doped system, the bulk bands contribution starts as early as 0.09 eV, leading to a lower spin polarisation. Therefore, for biases lower than 0.17 V, the B-doped DB wire drawn on H-passivated Si(100) system is a perfect non-leaking spin-filtering surface interconnect.

4. Conclusion

In summary, we have shown that boron and phosphorous dopants segregates to the H-passivated Si(100) surface. This phenomenon is enhanced by the presence of DB wires. The first effect of dopants is to stabilize the magnetic form of DB wires over the non-magnetic Peierls distorted one. As observed in other doped Si systems, the extra charge brought by the dopant is captured by the DB wire. One consequence is the closing of the electronic gap leading to quasi-metallicity of AFM DB wires. Moreover, the presence of dopants induce a total magnetic moment on the electronic bands close to the Fermi energy, leading to spin-specific electron transport. In the case of B-doped AFM DB wire, the current is not only free of leakage from the wire but also spin-specific. Therefore, B-doped DB wires are perfect spin-filtering surface interconnects.

Acknowledgments

This work has been supported by the European Union Integrated Project AtMol (<http://www.atmol.eu>). R. Rurali acknowledges funding under contract Nos. FEDER-FIS2012-37549-C05-05 and CSD2007-00041 of the Ministerio de Economía y Competitividad (MINECO). R. Robles and N. Lorente acknowledge financial support from Spanish MINECO (Grant No. MAT2012-38318-C03-02 with joint nancing by FEDER Funds from the European Union).

References

- [1] R. Jansen. Silicon spintronics. *Nature Mater.*, 11:400, 2012.
- [2] S. Sanvito. Molecular spintronics. *Chem. Soc. Rev.*, 40:3336, 2011.
- [3] A. R. Rocha, V. M. García-Suárez, S. W. Bailey, C. J. Lambert, J. Ferrer, and S. Sanvito. Towards molecular spintronics. *Nature Mater.*, 4:335, 2005.
- [4] L. Bogani and W. Wernsdorfer. Molecular spintronics using single-molecule magnets. *Nature Mater.*, 7:179, 2008.
- [5] A. Aviram and M. A. Ratner. Molecular rectifiers. *Chem. Phys. Lett.*, 29:277, 1974.
- [6] C. Joachim, J. K. Gimzewski, and A. Aviram. Electronics using hybrid-molecular and mono-molecular devices. *Nature*, 408:541, 2000.
- [7] M. Kepenekian, R. Robles, C. Joachim, and N. Lorente. Surface-state engineering for interconnects on h-passivated si(100). *Nano Lett.*, 13:1192, 2013.
- [8] S. Iijima. Helical microtubules of graphitic carbon *Nature*, 354:56, 1991.
- [9] J.-C. Charlier, X. Blase, and S. Roche. Electronic and transport properties of nanotubes. *Rev. Mod. Phys.*, 79:677, 2007.
- [10] Y. Cui, , and C. M. Lieber. Functional nanoscale electronic devices assembled using silicon nanowire building blocks. *Science*, 291:851, 2001.
- [11] R. Rurali. Colloquium: Structural, electronic, and transport properties of silicon nanowires. *Rev. Mod. Phys.*, 82:427–449, 2010.
- [12] B. Weber, S. Mahapatra, H. Ryu, S. Lee, A. Fuhrer, T. C. G. Reusch, D. L. Thompson, W. C. T. Tee, G. Klimeck, L. C. L. Hollenberg, and M. Y. Simmons. Ohms law survives to the atomic scale. *Science*, 335:64, 2012.
- [13] T.-C. Shen, C. Wang, G. C. Abeln, J. R. Tucker, J. W. Lyding, P. Avouris, and R. E. Walkup.

- Atomic-scale desorption through electronic and vibrational excitation mechanisms. *Science*, 268:1590, 1995.
- [14] S. Hosaka, S. Hosoki, T. Hasegawa, H. Koyanagi, T. Shintani, and M. Miyamoto. Fabrication of nanostructures using scanning probe microscopes. *J. Vac. Sci. Technol. B*, 13:2813, 1995.
- [15] T. Hitosugi, S. Heike, T. Onogi, T. Hashizume, S. Watanabe, Z.-Q. Li, K. Ohno, Y. Kawazoe, T. Hasegawa, and K. Kitazawa. Jahn-teller distortion in dangling-bond linear chains fabricated on a hydrogen-terminated si(100)-2x1 surface. *Phys. Rev. Lett.*, 82:4034, 1999.
- [16] L. Soukiassian, A. J. Mayne, M. Carbone, and G. Dujardin. Atomic wire fabrication by stm induced hydrogen desorption. *Surf. Sci.*, 528:121, 2003.
- [17] T. Hallam, T. C. G. Reusch, L. Oberbeck, N. J. Curson, and M. Y. Simmons. Scanning tunneling microscope based fabrication of nano- and atomic scale dopant devices in silicon: The crucial step of hydrogen removal. *J. Appl. Phys.*, 101:034305, 2007.
- [18] M. B. Haider, J. L. Pitters, G. A. DiLabio, L. Livadaru, J. Y. Mutus, and R. A. Wolkow. Controlled coupling and occupation of silicon atomic quantum dots at room temperature. *Phys. Rev. Lett.*, 102:046805, 2009.
- [19] J. L. Pitters, L. Livadaru, M. B. Haider, and R. A. Wolkow. Tunnel coupled dangling bond structures on hydrogen terminated silicon surfaces. *J. Chem. Phys.*, 134:064712, 2011.
- [20] S. Watanabe, Y. A. Ono, T. Hashizume, and Y. Wada. Theoretical study of atomic and electronic structures of atomic wires on an h-terminated si(100)-2x1 surfaces. *Phys. Rev. B*, 54:R17308, 1996.
- [21] S. Watanabe, Y. A. Ono, T. Hashizume, and Y. Wada. First-principles study of atomic wires on a h-terminated si (100)-(2x1) surface. *Surf. Sci.*, 386:340, 1997.
- [22] P. Doumergue, L. Pizzagalli, C. Joachim, A. Altibelli, and A. Baratoff. Conductance of a finite missing hydrogen atomic line on si(001)-2x1-h. *Phys. Rev. B*, 59:15910, 1999.
- [23] J.-H. Cho and L. Kleinman. Nature of lattice distortion in one-dimensional dangling-bond wires on si and c. *Phys. Rev. B*, 66:235405, 2002.
- [24] C. F. Bird, A. J. Fisher, and D. R. Bowler. Soliton effects in dangling-bond wires on si(001). *Phys. Rev. B*, 68:115318, 2003.
- [25] M. Çakmak and G. P. Srivastava. Theoretical study of dangling-bond wires on the h-terminated si surfaces. *Surf. Sci.*, 532-535:556, 2003.
- [26] J. Y. Lee, J.-H. Choi, and J.-H. Cho. Antiferromagnetic coupling between two adjacent dangling bonds on si(001): Total-energy and force calculations. *Phys. Rev. B*, 78:081303, 2008.
- [27] J. Y. Lee, J.-H. Cho, and Z. Zhang. Quantum size effects in competing charge and spin orderings of dangling bond wires on si(001). *Phys. Rev. B*, 80:155329, 2009.
- [28] H. Kawai, Y. K. Yeo, M. Saeys, and C. Joachim. Conductance decay of a surface hydrogen tunneling junction fabricated along a si(001)-(2x1)-h atomic wire. *Phys. Rev. B*, 81:195316, 2010.
- [29] J.-H. Lee and J.-H. Cho. Instability of one-dimensional dangling-bond wires on h-passivated c(001), si(001), and ge(001) surfaces. *Surf. Sci.*, 605:L13, 2011.
- [30] R. Robles, M. Kepenekian, S. Monturet, C. Joachim, and N. Lorente. Energetics and stability of dangling-bond silicon wires on h-passivated si(100). *J. Phys.: Condens. Matter*, 24:445004, 2012.
- [31] M. Kepenekian, F. D. Novaes, R. Robles, S. Monturet, H. Kawai, C. Joachim, and N. Lorente. Electron transport through dangling-bond silicon wires on h-passivated si(100). *J. Phys.: Condens. Matter*, 25:025503, 2013.
- [32] A. J. Schofield, P. Studer, C. F. Hirjibehedin, N. J. Curson, G. Aeppli, and D. R. Bowler. Quantum engineering at the silicon surface using dangling bonds. *Nat. Commun.*, 4:1649, 2013.
- [33] M. Kepenekian, R. Robles, C. Joachim, and N. Lorente. Leakage current in atomic-size surface interconnects. *Appl. Phys. Lett.*, 103:161603, 2013.
- [34] J. M. Soler, E. Artacho, J. D. Gale, A. García, J. Junquera, P. Ordejón, and D. Sánchez-Portal. The siesta method for ab initio order-n materials simulation. *J. Phys.: Condens. Matter*,

- 14:2745, 2002.
- [35] E. Artacho, E. Anglada, O. Diéguez, J. D. Gale, A. García, J. Junquera, R. M. Martin, P. Ordejón, J. M. Pruneda, D. Sánchez-Portal, and J. M. Soler. The siesta method; developments and applicability. *J. Phys.: Condens. Matter*, 20:064208, 2008.
 - [36] J. P. Perdew, K. Burke, and M. Ernzerhof. Generalized gradient approximation made simple. *Phys. Rev. Lett.*, 77:3865, 1996.
 - [37] N. Troullier and J. L. Martins. Efficient pseudopotentials for plane-wave calculations. *Phys. Rev. B*, 43:1993, 1991.
 - [38] E. Artacho, D. Sánchez-Portal, P. Ordejón, A. García, and J. M. Soler. Linear-scaling ab-initio calculations for large and complex systems. *phys. stat. sol. (b)*, 215:809, 1999.
 - [39] M. Brandbyge, J.-L. Mozos, P. Ordejón, J. Taylor, and K. Stokbro. Density-functional method for nonequilibrium electron transport. *Phys. Rev. B*, 65:165401, 2002.
 - [40] S. Datta. *Electronic Transport in Mesoscopic Systems*. Cambridge University Press, 2007.
 - [41] X. Luo, S. B. Zhang, and S.-H. Wei. Understanding ultrahigh doping: The case of boron in silicon. *Phys. Rev. Lett.*, 90:026103, 2003.
 - [42] S. A. Centoni, B. Sadigh, G. H. Gilmer, T. Díaz de la Rubia, and C. B. Musgrave. First-principles calculation of free si(100) surface impurity enrichment. *Appl. Phys. Lett.*, 87:232101, 2005.
 - [43] M. V. Fernández-Serra, Ch. Adessi, and X. Blase. Surface segregation and backscattering in doped silicon nanowires. *Phys. Rev. Lett.*, 96:166805, 2006.
 - [44] H. Peelaers, B. Partoens, and F. M. Peeters. Formation and segregation energies of b and p doped and bp codoped silicon nanowires. *Nano Lett.*, 6:2781, 2006.
 - [45] M. V. Fernández-Serra, Ch. Adessi, and X. Blase. Conductance, surface traps, and passivation in doped silicon nanowires. *Nano Lett.*, 6:2674, 2006.